Low-temperature synthesis of large-scale arrays of aligned tungsten oxide nanorods

2003 J. Phys.: Condens. Matter 15 L453

(http://iopscience.iop.org/0953-8984/15/29/101)

INSTITUTE OF PHYSICS PUBLISHING JOURNAL OF PHYSICS: CONDENSED MATTER

J. Phys.: Condens. Matter **15** (2003) L453–L461 PII: S0953-8984(03)61930-2

LETTER TO THE EDITOR

Low-temperature synthesis of large-scale arrays of aligned tungsten oxide nanorods

Jingguo Liu, Ye Zhao and Zhengjun Zhang[1]

Department of Materials Science and Engineering, Tsinghua University, Beijing 100084, People's Republic of China

E-mail: zjzhang@tsinghua.edu.cn

Received 13 June 2003
Published 11 July 2003
Online at stacks.iop.org/JPhysCM/15/L453

Abstract

We report, in this letter, a simple thermal oxidation approach to growing large-scale arrays of aligned tungsten oxide nanorods on planar substrates. By passing a current of ∼50 A through a tungsten spiral coil in a vacuum of $\sim 3 \times 10^{-2}$ Torr, single-crystalline $WO_{2.9}$ nanorods, ∼20 nm in diameter and ∼400 nm long, were deposited on planar substrates, e.g. Si(001), Si(111), SiO_2/Si, glass, and Ag-coated silicon substrates at temperatures below 200 °C. The nanorods were vertically aligned on the substrates. The structure, optical properties and alignment of the nanorods was investigated by x-ray diffraction and transmission electron microscopes, micro-Raman spectrometer, and scanning electron microscope and x-ray pole figure measurement, respectively. The present study provides an easy way to grow large-scale arrays of aligned tungsten oxide nanorods at relatively low temperatures, which might also be applicable to the growth of other metal oxides.

Materials of low dimensionality, such as nanotubes [1], microtubes [2], nanowires [3], nanobelts [4], nanoribbons [5], nanorods [6] and microrods [7], exhibit various outstanding properties that are attractive to nanotechnology and have thus stimulated enormous research interest in the past decade. For instance, carbon nanotubes are a very promising candidate material for applications in future devices, such as high-resolution field emission flat displays [8], miniature x-ray sources [9], molecular, single-electron transistors and logic circuits [10], units for molecular computing [11] and nanotools [12], etc. Therefore, the preparation and controlled growth, structure characterization and property evaluation of materials with reduced sizes have become the research focus in the field in recent years [1–4, 13].

Transition metal oxides are a large family of materials possessing various interesting properties such as superconductivity, colossal magneto-resistance and piezoelectricity, etc.

[1] Author to whom any correspondence should be addressed.

0953-8984/03/290453+09$30.00

Transition metal oxides with size reduced down to the nanometre scale, are promising materials for applications in lithium-ion batteries, catalysts, electrochromic materials and sensors due to their huge surface areas [14–16]. Thus much research effort has been stimulated and directed to developing new approaches to synthesizing materials of reduced dimensions, and to the investigation of their structure, properties and the structure–property relationship on the nanometre scale [17–20].

WO_x exhibits excellent photo- and electrochromic properties and can be applied as semiconductor sensors. However, due to lack of preparation methods, studies on the nanosized WO_x materials are still rare. It has been reported recently that, by heating a tungsten tip in Ar atmosphere at ∼700 °C, isolated tungsten oxide nanowires can be grown directly on the tungsten tip [21]. This provides a simple way to prepare nanosized WO_x. However, the tungsten oxide nanowires so produced were grown at a relatively high temperature, i.e. 700 °C, and were not grown and aligned on planar alien substrates like Si, which is a necessity for their application to devices. Therefore, new methodologies are highly in demand for the preparation of aligned nanosized WO_x materials on planar substrates at low temperatures.

In this letter, we describe a simple thermal oxidation method to fabricate large-scale arrays of aligned tungsten oxide nanorods on planar substrates at low temperatures and the investigation of the structure, alignment and optical properties of the nanorods.

A spiral coil (∼2 cm in diameter and ∼5 cm long) was made with a tungsten wire of a purity of 99.9% and connected to two copper electrodes in a vacuum chamber. A series of planar substrates, e.g. 3°-cut Si(001), Si(111), SiO_2/Si, glass and Ag-coated Si substrates, were cleaned ultrasonically in acetone, alcohol and deionized water in sequence and were fixed on a substrate holder ∼5 cm above the coil. The chamber was first pumped down to $\sim 3 \times 10^{-2}$ Torr, and then a voltage (adjusted by a voltage regulator connected to a voltage changer) was applied to the two copper electrodes, resulting in a current passing through the tungsten coil, rapidly heating up the coil. Due to the oxidation of the tungsten coil, arrays of aligned tungsten oxide nanorods were deposited on the substrates. The temperature of the substrates was measured with a thermocouple and was found to be below ∼200 °C within a typical deposition time of ∼1 min. The temperature of the tungsten spiral coil was monitored with a WFH-655 fibre optic infrared thermometer working at temperatures ranging from 600 to 2000 °C. The advantage of this approach is the easy control of the nanorods' growth via adjusting the voltage applied to the two electrodes or, equivalently, the current passing through the coil. Electron microscopes (scanning electron microscope (SEM), transmission electron microscope (TEM)), x-ray diffraction, x-ray pole figure measurement and a micro-Raman spectrometer were employed to observe the morphology of the deposits on the substrate, to characterize the structure and to evaluate the properties of the deposits, respectively.

When passing a current of ∼50 A through the tungsten coil for ∼1 min, large-scale tungsten oxide nanorods have been deposited on all substrates used, i.e. 3°-cut Si(001), Si(111), SiO_2/Si, glass and Ag-coated silicon. The temperature of the coil, as monitored by the fibre optic infrared thermometer, was ∼850 °C. Figure 1 shows SEM micrographs of the tungsten oxide nanorods grown on the 3°-cut Si(001) substrate, taken with a JSM-6301F field emission SEM working at 20 kV. One sees from figures 1(a) and (b) that tungsten oxide nanorods have been grown in large scale on the substrate. The nanorods, as shown by figures 1(c) and (d), are ∼20 nm in diameter and ∼400 nm in length, and are well aligned with each other (figure 1(c)). One sees also from figure 1(d) that, for the majority of the nanorods, their axis is almost parallel to the surface normal of the silicon substrate.

X-ray diffraction analysis has been performed to identify the structure of the tungsten oxide nanorods. Figure 2 is a typical x-ray diffraction pattern of the large-scale arrays of nanorods, taken with a Rigaku diffractometer at a scan step of 0.02°, using Cu Kα radiation. The reason

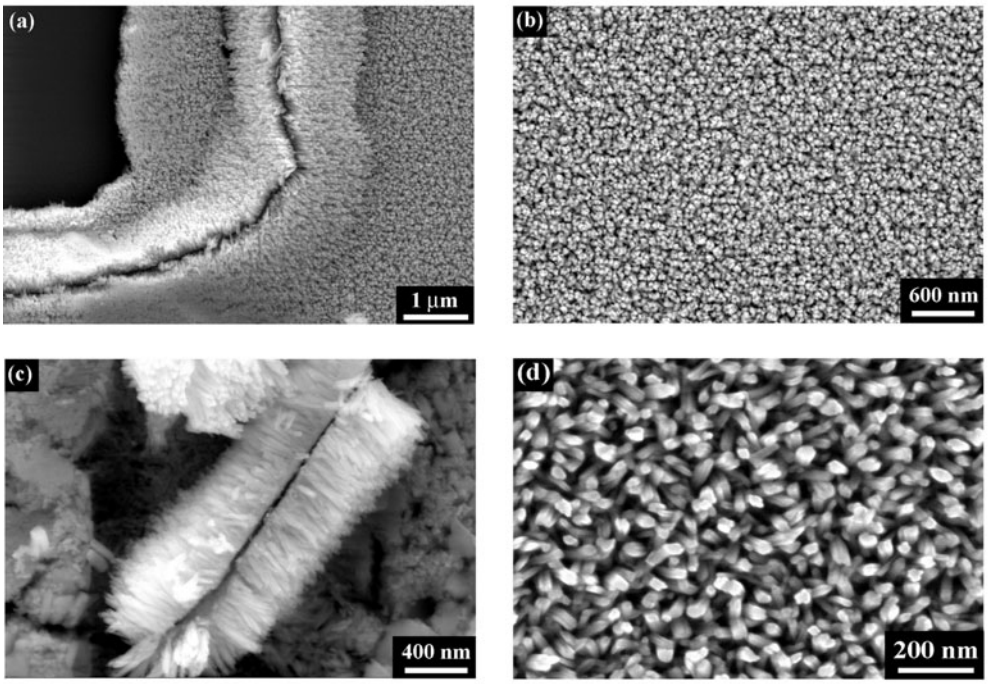

Figure 1. SEM images of tungsten oxide nanorods deposited on the Si(001) substrate at a current of ∼50 A for ∼1 min. (a) and (b) are low-magnification views showing the surface morphology in large scale; (c) and (d) are high-magnification cross section and top views, showing the alignment of the nanorods.

that we used a 3°-cut Si(001) substrate is to avoid the overlapping of the Si peaks with the peaks of the deposits, which might result in difficulties in phase identification. Obviously, the intensity of the Si(004) peak in the patterns was drastically decreased. The pattern shows clearly the (010), (020) and (030) diffractions of a single phase of $WO_{2.9}$, with a monoclinic structure [22], suggesting that the deposits are $WO_{2.9}$ nanorods. Since no other diffraction peaks of the $WO_{2.9}$ phase were observed in the pattern, for the majority of the tungsten oxide nanorods, their axis should be along $[010]_{WO_{2.9}}$. Considering both the x-ray diffraction analysis and SEM analysis shown in figure 1(d), it is suggested that, for most nanorods, their fabric axis is along $[010]_{WO_{2.9}}$ and is almost parallel to the surface normal of the substrate, i.e. $[010]_{WO_{2.9}} \parallel [001]_{Si}$.

We have performed TEM and HRTEM analysis of individual nanorods to examine the structure and deposition axis of the nanorods. Figures 3(a) and (b) show a typical bright field image of several nanorods and a selected area diffraction (SAD) of the nanorods, respectively. The image and SAD pattern were taken with a JEOL-200 CX TEM working at 200 kV. It is seen that the diameter of the nanorods is ∼20 nm and that the nanorods are single crystalline. The reason that the SAD pattern shows lines rather than spots along directions perpendicular to the deposition axis is probably due to the reduced dimension of the nanorods that causes a corresponding extension in the reciprocal space. Figure 3(c) shows a typical HRTEM image of an individual nanorod taken with a JEM-2010F TEM working at 200 kV. From this figure one sees clearly that the $WO_{2.9}$ nanorod is single crystalline and that the deposition axis of the nanorod is along the $[010]_{WO_{2.9}}$ direction, which is in good agreement with the x-ray diffraction analysis.

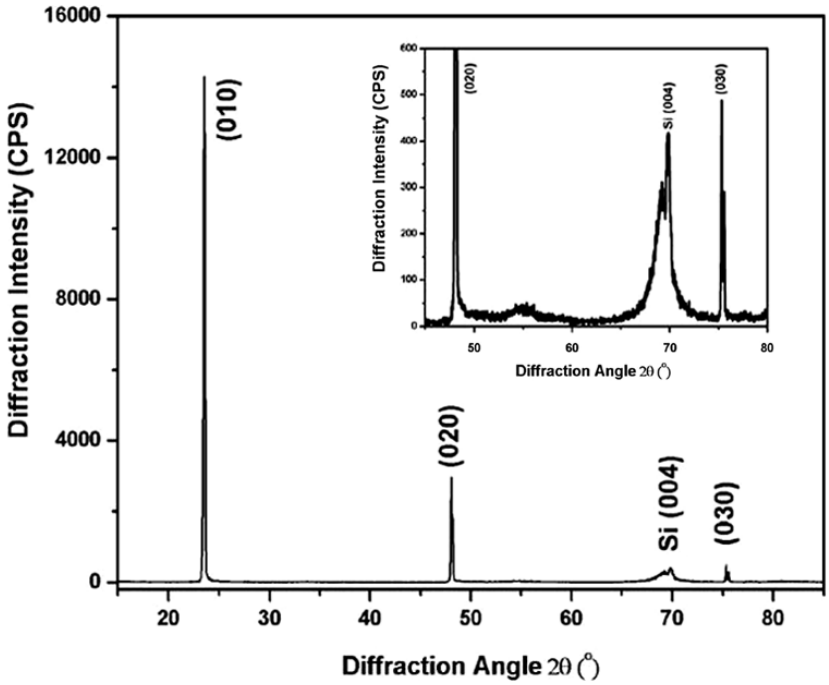

Figure 2. The x-ray diffraction pattern of the nanorods. Inset is an enlarged part of the pattern with (020) and (030) diffraction peaks.

The alignment of the nanorods was evaluated by x-ray pole figure measurements. Figure 4 shows the (010) pole figure of the $WO_{2.9}$ nanorods. The pole figure was obtained by fixing the detector at the (010) diffraction position of $2\theta = 23.52°$ and measuring the intensity change of the (010) diffraction in the reciprocal space, by tilting the sample from 0° to 75° at a step of 2° and rotating the sample from 0° to 360° at a step of 5°, respectively. The measurement gives, in other words, information on the distribution of the deposition axis of the nanorods, i.e. $[010]_{WO_{2.9}}$, in real space. We see that the intensity of the (010) diffraction was localized around the central area of the pole figure, with a full width at half-maximum (FWHM) of the pole figure narrower than 5°. This suggests that, for the majority of the nanorods, their deposition axis, i.e. $[010]_{WO_{2.9}}$, is almost parallel. That is to say, the nanorods are well aligned. Therefore, the x-ray pole figure measurement can be a way to evaluate the alignment of one-dimensional materials like nanorods and nanotubes. Since the central spot of the pole figure is the surface normal of the substrate, the distribution of the (010) diffraction of the nanorods around the central spot with a FWHM of $<5°$ implies also an orientation relationship of $[010]_{WO_{2.9}} \parallel [001]_{Si}$ between the nanorods and the substrate. We have also performed pole figure measurements for other diffractions, yet could not find any other texture. Thus the only orientation relationship among $WO_{2.9}$ nanorods deposited on the Si(001) substrate is their parallel deposition axis, i.e. $[010]_{WO_{2.9}}$, which can be described by a deposition texture of $[010]_{WO_{2.9}} \parallel [001]_{Si}$ or $(010)_{WO_{2.9}} \parallel (001)_{Si}$, as indicated by the pole figure shown in figure 4. The optical properties of the arrays of the $WO_{2.9}$ nanorods were examined by a micro-Raman spectrometer. Figure 5 is a typical Raman spectrum of the $WO_{2.9}$ nanorods excited by a 488 nm Ar^+ laser, showing a broad peak around 800–900 cm^{-1}, which is in agreement with the nanosized nature of the $WO_{2.9}$ [23].

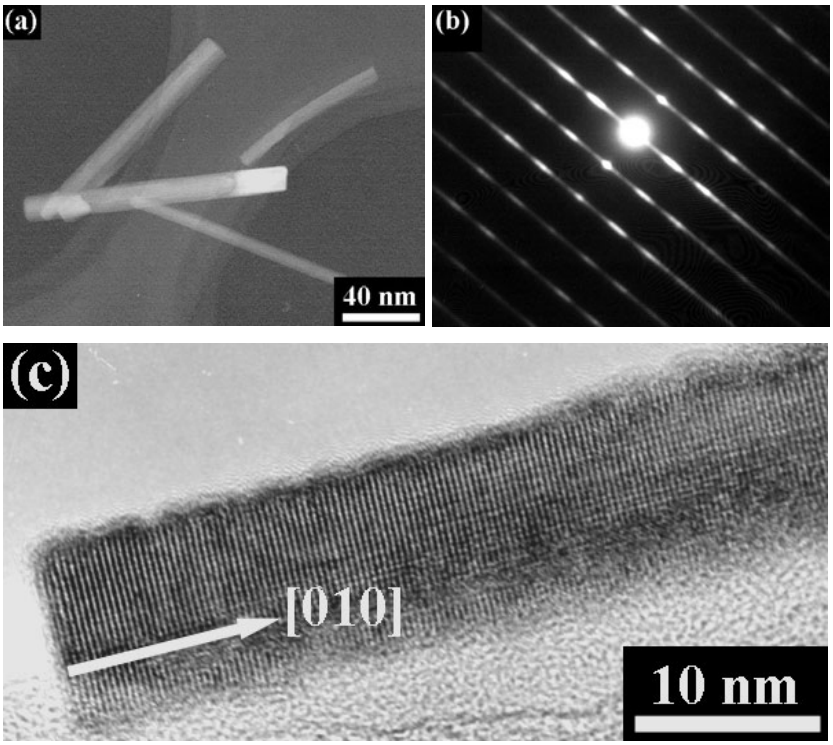

Figure 3. TEM analysis of the tungsten oxide nanorods: (a) a typical low-magnification bright field image of the nanorods; (b) a typical SAD pattern of the nanorods; and (c) a typical HRTEM image of an individual nanorod.

The x-ray pole figure shown in figure 4 suggests not only that the nanorods are well aligned with each other but also that there is an orientation relationship between the nanorods and the substrate, i.e. $[010]_{WO_{2.9}} \parallel [001]_{Si}$ or $(010)_{WO_{2.9}} \parallel (001)_{Si}$. However, the (001) spacing of Si and (010) of $WO_{2.9}$ is 1.36 and 3.36 Å, respectively. It is thus very hard to establish an epitaxial relationship between them by this simple approach. We believe that the aligned growth of the $WO_{2.9}$ nanorods is similar to that of carbon nanotubes on planar substrates, i.e. the alignment was established via the crowding effect rather than a specific orientation relationship between the deposits and the substrate [24]. If this holds, the aligned growth of $WO_{2.9}$ nanorods should not be sensitive to the substrate and can be realized on other planar substrates. We therefore conducted experiments on a series of other substrates, e.g. Si(111), SiO_2/Si, glass and Ag-coated silicon substrates, etc. In all cases, aligned growth of the $WO_{2.9}$ nanorods has been observed at the same deposition conditions. Figure 6 compares the x-ray diffraction patterns of the nanorods deposited on Si(111) and SiO_2/Si(111) substrates, showing the vertically aligned growth on both substrates. HRTEM analysis and x-ray pole figure measurement (not shown) give the same results shown by figures 3 and 4. These suggest that the vertical alignment of the nanorods, similar to the aligned growth of carbon nanotubes on a planar substrate, is probably due to the crowding effect, rather than the establishment of a specific orientation relationship between the nanorods and the substrate. This approach therefore can be applied to depositing aligned $WO_{2.9}$ nanorods on a variety of planar substrates for different purposes.

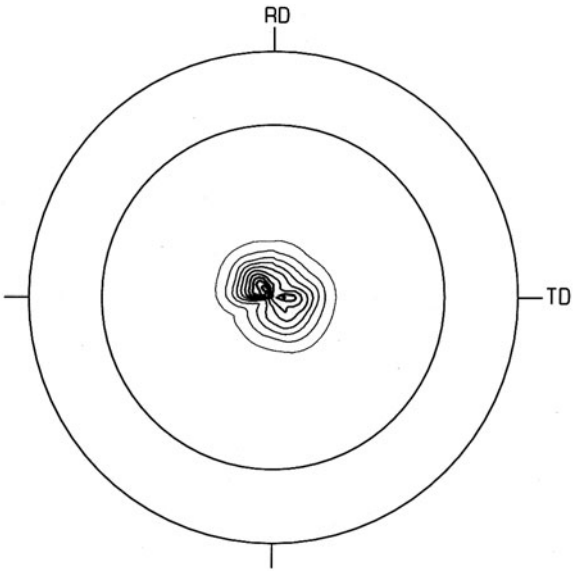

Figure 4. The (010) x-ray pole figure of the nanorods, showing the good parallelism of the deposition axis of the nanorods. The diffraction intensity was divided into 10 segments.

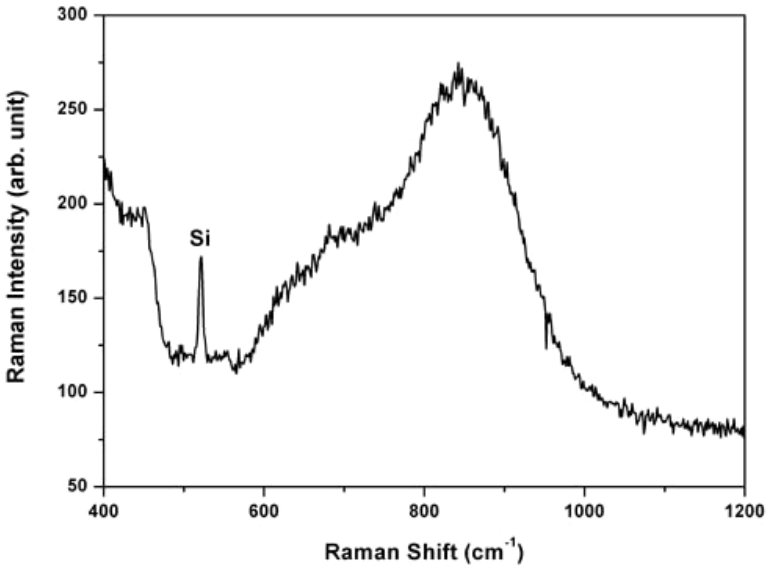

Figure 5. Raman spectrum of the tungsten oxide nanorods.

In addition, the growth might be influenced by the oxidation process of the tungsten coil, adjustable via controlling the current passing through the tungsten coil. We therefore investigated the influence of the current passing through the coil on the growth of the tungsten oxide nanorods. Figure 7 shows x-ray diffraction patterns of nanorods grown at different currents within a fixed growth time of ∼1 min. It shows that the growth of nanorods is very dependent on the current. At a current of ∼50 A, only $WO_{2.9}$ nanorods were deposited, while

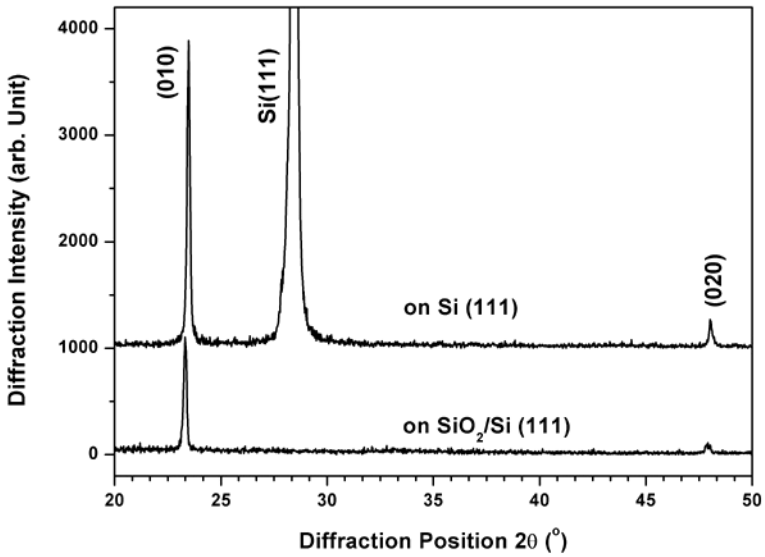

Figure 6. X-ray diffraction patterns of the nanorods grown on the Si(111) and SiO_2/Si(111) substrates.

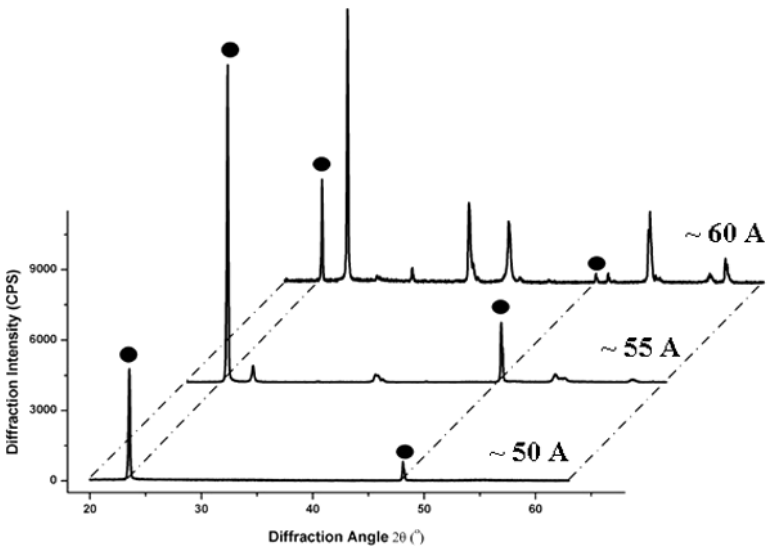

Figure 7. X-ray diffraction patterns of the nanorods grown at a current of ∼50, 55 and 60 A. The growth time was fixed at ∼1 min. The full circles represent diffractions of $WO_{2.9}$ nanorods, while other peaks are diffractions of WO_2 nanorods.

at currents $\geqslant$55 A, WO_2 nanorods were also observed. In the deposits produced at a current of ∼60 A, the WO_2 nanorods became dominant. This is because, in the authors' view, a higher current heats up the coil to a higher temperature, leading to faster oxidation of the tungsten coil and requiring more oxygen atoms to form $WO_{2.9}$, while the supply of the oxygen atoms is limited in a vacuum of $\sim 3 \times 10^{-2}$ Torr, thus resulting in the formation of WO_2 nanorods

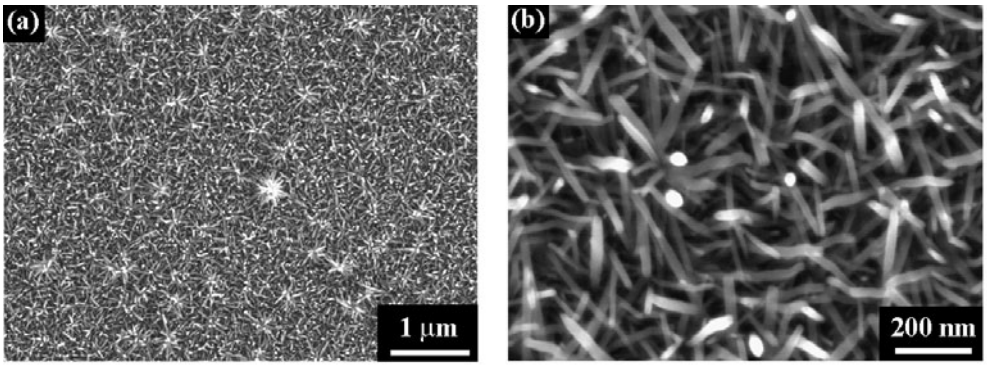

Figure 8. Influence of surface cleanliness on the alignment of $WO_{2.9}$ nanorods deposited on the Si(001) substrates. The current is ∼50 A and the deposition time is ∼1 min.

rather than $WO_{2.9}$. The coil temperature at currents of ∼50, 55 and 60 A was measured by the fibre optic infrared thermometer to be ∼850, 1100 and 1450 °C, respectively.

Another factor that influences the growth of the tungsten oxide nanorods we have investigated is the cleanliness of the substrate surface. Figure 8 shows SEM images of $WO_{2.9}$ nanorods grown on a Si(001) substrate not supersonically cleaned at a current of ∼50 A for ∼1 min. X-ray diffraction analysis (not shown) indicates that they are $WO_{2.9}$ nanorods, similar to those deposited on a ultrasonically cleaned substrate. Comparing figures 8 and 1, the only difference is the alignment of the nanorods. The nanorods grown on the substrate not ultrasonically cleaned, as shown by figure 8, are of diameters and lengths similar to those grown on the cleaned substrate (figure 1). However, in comparison with those grown on a cleaned substrate (figure 1(d)), the nanorods grown on the uncleaned substrate lost the alignment (figure 8(b)).

To summarize, we have developed a thermal oxidation method to produce arrays of aligned tungsten oxide nanorods in a large scale. By this means the current passing through the tungsten coil played a key role in the phase selection of the tungsten oxide to grow, and the cleanliness of the substrate surface determined the alignment of the nanorods. The alignment of the nanorods is probably due to the crowding effect rather than establishing a specific orientation relationship with the substrate. This study provides a simple way to prepare aligned tungsten oxides nanorods on planar substrates for different purposes.

The authors are grateful to the financial support by the Chinese National Natural Science Foundation (50225102, 50201008), the support of the Ministry of Science and Technology of China (2002CB613501), and the support from the Ministry of Education of China (200133).

References

[1] Iijima S 1991 *Nature* **354** 56
[2] Vayssieres L, Keis K, Hagfeldt A and Lindquist S E 2001 *Chem. Mater.* **13** 4395
[3] Morales A M and Lieber C M 1998 *Science* **279** 208
Zhang Y F *et al* 1998 *Appl. Phys. Lett.* **72** 1835
Duan X F, Huang Y, Wang J F and Lieber C M 2001 *Nature* **409** 66
[4] Pan Z W, Dai Z R and Wang Z L 2001 *Science* **291** 1947
[5] Shi W S *et al* 2001 *J. Am. Chem. Soc.* **123** 11095
[6] Dai H J, Wong E W, Lu Y Z, Fan S S and Lieber C M 1995 *Nature* **375** 769
Han W Q, Fan S S, Li Q Q and Hu Y D 1997 *Science* **277** 1287

[7] Vayssieres L, Keis K, Lindquist S E and Hagfeldt A 2001 *J. Phys. Chem.* B **105** 3350
[8] Deheer W A, Chatelain A and Ugarte D 1995 *Science* **270** 1179
Fan S S *et al* 1999 *Science* **283** 512
[9] Yue G Z *et al* 2002 *Appl. Phys. Lett.* **81** 355
[10] See, for example, Tans S J, Verschueren A R M and Dekker C 1998 *Nature* **393** 49
[11] See, for example, Rueckes T *et al* 2000 *Science* **289** 94
[12] Kim P and Lieber C M 1999 *Science* **286** 2148
Gao Y H and Bando Y 2002 *Nature* **415** 599
[13] Liang L, Liu J, Windisch C F Jr, Exarhos G J and Lin Y 2002 *Angew. Chem., Int. Edn Engl.* **41** 3665
Tian Z, Voigt J A, Liu J, Mckenzie B and Mcdermott M J 2002 *J. Am. Chem. Soc.* **124** 12954
Liu J *et al* 2003 *Chem. Eur. J.* **9** 604
[14] Poizot P, Grugeon S, Dupont L and Tarascon J-M 2000 *Nature* **407** 496
[15] Ponzi M, Duschatzky C, Carrascull A and Ponzi E 1998 *Appl. Catal.* A **169** 373
[16] Talledo A and Granqvist C G 1995 *J. Appl. Phys.* **77** 4655
[17] Choi Y C *et al* 2000 *Adv. Mater.* **12** 746
[18] Morales A M and Lieber C M 1998 *Science* **279** 208
[19] Yang P and Lieber C M 1996 *Science* **273** 1836
[20] Bai Z G *et al* 1999 *Chem. Phys. Lett.* **303** 311
[21] Gu G, Zheng B, Han W Q, Siegmar R and Liu J 2002 *Nano Lett.* **2** 829
[22] JCPDS Card, No 36-0102
[23] Frey G L *et al* 2001 *J. Solid State Chem.* **162** 300
[24] Zhang Z J, Wei B Q, Ramanath G and Ajayan P M 2000 *Appl. Phys. Lett.* **77** 3764